

NUMERICAL SOLUTION OF ELLIS FLUID MODEL IN STENOSED ARTERIES

REKHA BALI, NIVEDITA GUPTA* AND SWATI MISHRA

Department of Mathematics, HBTU, Kanpur - 208002, India.

Received On: 09-06-17; Revised & Accepted On: 30-06-17)

ABSTRACT

The aim of this paper is to develop mathematical model for studying the non-Newtonian flow of blood through a blood vessels. Ellis fluid has been taken to represent the non-newtonian character of blood. The problem is solved by using numerical and analytical techniques with the help of boundary conditions. Results are displayed graphically for different flow characteristics like flow rate, skin friction and resistance to flow. The results are compared with data available in the existing literature presented by previous research.

Keywords: Ellis Fluid; stenosis; flow rate; resistance to flow; skin friction.

7.1 INTRODUCTION

The study of flow of non-Newtonian fluid through small vessels has been the subject of extensive investigations because of the velocity of applications such as chemical, environmental and biomedical engineering. Non-Newtonian fluids are well described by the Power-law model, Ellis Model, Herschel-Bulkley model, Casson model etc. All these models describe the flow of blood in small vessels. Ellis model has the advantage of being able to describe the fluid flow behavior over a greater range of shear rates than the power law model. But it has also a disadvantage in that the least squares fit necessary for the experimental data needs a complex computer program. At very low shear rates, the model reduces to Newtonian behavior while at high shear rates; the model approaches a power-law model. Hence, Ellis fluid model is really a combination of the two. The power law kinematic viscosity is taken only in the momentum equations while the thermal conductivity is taken the same as in the Newtonian fluids.

The mechanics of non-Newtonian fluids are important to engineers, modeler numerical analyst and mathematicians. The flows of non Newtonian fluids are not only important because of their technological significance but also due to the interesting mathematical features presented by their governing equations. The rheological behavior of non-Newtonian fluids is very complex and it is not possible to find a universal constitutive relation valid for all non-Newtonian fluids. The main advantage of Ellis equation is that it predicts the Newtonian behavior at small shear stresses and the power law behavior at large shear stresses.

Several researchers work on stenosed artery with different non-Newtonian fluid (Chaturani & Kalone 1976, Chaturani & Upadhyay 1979, Shukla *et al.* 1980, Majhi & Usha 1984, Chaturani & Biswas 1983, Philip and Chandran 1996) have theoretically studied the flow of blood uniform and stenosed tubes. Chaturani and Samy analyzed the pulsatile flow of casson fluid through stenosed artery using perturbation method (1986). Prahlad and Schultz (2004) developed a model of blood flow in a stenosed tube. In their paper blood is considered as couple stress fluid. They discussed the rheological properties such as velocity, resistance to flow and shear stress for different hematocrit suspension and for the disease of blood like polycythemia, plasma cell dyscrasia and sickle cell. After that Mishra and shit (2006) develop a mathematical model for studying the Herschel-Bulkley fluid through a stenosed arterial segment. Venkatesan *et al.* (2013) studied the casson fluid model through a narrow artery with bell shaped stenosis. They compared their results with the results of Misra and shit (2006). It is also noticed that resistance to flow and skin friction increase with the increase of the yield stress.

In 2007 R. Ponalagusammy is developed a two layered model for blood flow with different shapes of stenosis. Two layered defined as core layer (region) is surrounded by peripheral layer (region). Shit *et al.* (2012) presents the mathematical model of blood flow through a tapered overlapping stenosed artery with variable viscosity. The blood is considered as porous in nature. They obtained the result for volumetric flow rate, velocity component, wall shear stress and pressure gradient with the effect of hematocrit magnetic field and the shape of artery.

Corresponding Author: Nivedita Gupta*,
Department of Mathematics, HBTU, Kanpur - 208002, India.

Ellahi *et al.* (2014) developed model for blood flow of nanofluids through an artery with composite stenosis and permeable wall. In their model the equation of nanoparticle and temperature are coupled. Prasad *et al.* (2014) considered a mathematical model of steady flow of Herschel-Bulkely fluid through an overlapping stenosis. They also developed the expression for resistance to flow and wall shear stress. After that they finalized the result that the HB fluid model is more appropriate to the stenosis than the Newtonian fluid. Further Nadeem and Ijaz in (2015) studied the theoretical analysis of metallic nanoparticles on blood flow through stenosed artery with permeable walls. They obtained the pressure gradient and resistance to flow in the stenotic region.

All the above cited investigations cover the flow of different non-newtonian fluid in stenotic blood vessels. However there is no attempt is available using Ellis fluid while Ellis model has the advantage of being able to describe the flow behavior over a greater range of shear rates than Power law model. Therefore our aim is to study the Ellis fluid model in stenosed artery.

7.2 FORMULATION OF THE PROBLEM

Consider a polar coordinate system (r', θ', z') where r' and z' are along the radius of an artery and along the length of an artery respectively and θ' represents the circumferential direction. A circular artery with radius R_0 and length $2L$ is considered as in figure 7.1. Blood is considered as an Ellis fluid in stenosed artery. Since the blood flow in artery is slow and steady, so magnitude and inertial forces are negligible and only one component of velocity parallel to the z' -axis. ρ is the density of fluid and u_0 is the blood velocity.

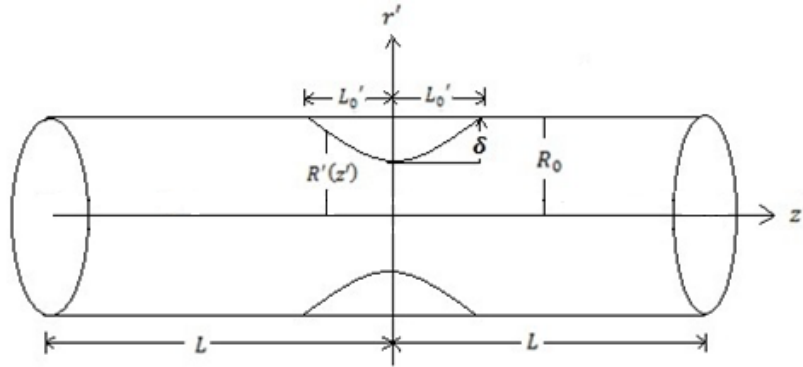


Fig. 7.1 Geometry of the arterial segment with stenosis

The bell-shaped mild stenosis in an artery is studied and the geometry of segment of artery with mild bell-shaped stenosis is shown in figure 1 and is defined as follows:

$$R'(z') = R_0 \left(1 - ae^{-bz'^2} \right) \quad (7.1)$$

where $R'(z')$, R_0 are the radius of an artery with and without stenosis respectively; a and b are non dimensional parameters defined as $a = \frac{\delta}{R_0}$, $b = \frac{m^2}{L_0^2}$; δ is the stenosis height, m represents the shape of stenosis and $2L_0$ is the length of stenosis.

The governing momentum equation is

$$\frac{1}{r'} \frac{d}{dr'} (r' \tau') = - \frac{dp'}{dz'} \quad (7.2)$$

where p' is the pressure at any point of an artery and τ' represents the shear stress of blood considered as Ellis Fluid.

The constitutive equation for Ellis fluid model is defined as follows:

$$\mu = \frac{\mu_0}{1 + \left(\frac{\tau'}{\tau'_{1/2}} \right)^{\alpha-1}} \quad (7.3)$$

Where μ_0 the low is shear viscosity, $\tau'_{1/2}$ is the shear stress at which $\mu = \mu_0 / 2$ and α is an indicial parameter in the model.

The volumetric flow rate can be expressed in terms of

$$Q'(r') = \frac{\pi R'^3}{\tau_R'^3} \int_{\tau_y'}^{\tau_R'} \tau'^2 f(\tau') d\tau' \quad (7.4)$$

Non-dimensional scheme are

$$z = \frac{z'}{L}, \quad r = \frac{r'}{R_0}, \quad u = \frac{u'}{u_0}, \quad R(z) = \frac{R'(z')}{R_0}, \quad p = \frac{p'}{\rho u_0^2}, \quad \tau = \frac{\tau'}{\rho u_0^2}.$$

7.3 SOLUTION OF THE PROBLEM

Solve equation (7.2) under the boundary condition, τ is finite at $r = 0$, we have

$$\tau = \frac{R_0}{L} \frac{r}{2} \frac{dp}{dz} \quad (7.5)$$

The skin friction is obtained as

$$\tau_R = -\frac{R_0}{L} \frac{R}{2} \frac{dp}{dz} \quad (7.6)$$

From equation (7.3), we find the most general form of Ellis model in non-dimensional form

$$f(\tau) = -\frac{du}{dr} = \frac{\rho u_0 R_0}{\mu_0} \tau \left[1 + \left(\frac{\tau}{\tau_{1/2}} \right)^{\alpha-1} \right] \quad (7.7)$$

Using equation (7.4) and (7.7) we obtain the volumetric flow rate in non dimensional form under the conditions $\tau_R \ll \tau_R^\alpha$

$$Q = \frac{\rho u_0 R_0}{4\mu_0} R^3 \tau_R \left[1 + \frac{4}{\alpha+3} \left(\frac{\tau_R}{\tau_{1/2}} \right)^{\alpha-1} \right] \quad (7.8)$$

Now we derive the equation for the skin friction from the above expression as

$$\tau_R = \left[\frac{Q}{\rho u_0 R_0} \frac{(\alpha+3)\mu_0}{R^3} \tau_{1/2}^{\alpha-1} \right]^{1/\alpha} \quad (7.9)$$

The resistance to blood flow is defined by

$$\lambda = \frac{p_0 - p_1}{Q} \quad (7.10)$$

where p_0 and p_1 are the pressures at the entry and the exit point of an artery respectively.

using equation (7.6), equation (7.9) can be written in the form

$$-\frac{dp}{dz} = \frac{2L}{RR_0} \left(\frac{Q}{\rho u_0 R_0} \frac{(\alpha+3)\mu_0}{R^3} \tau_{1/2}^{\alpha-1} \right)^{1/\alpha} \quad (7.11)$$

Integrating above equation under the condition that $p = p_1$ at $z = -1$ and $p = p_1$ at $z = 1$.

$$p_1 - p_2 = \frac{2L}{R_0^{1+\frac{1}{\alpha}}} \left(\frac{(\alpha+3)\mu_0 Q}{\rho u_0} \tau_{1/2}^{\alpha-1} \right)^{1/\alpha} [(2 - 2L_0) + I] \quad (7.12)$$

where $I = \int_{-L_0}^{L_0} \frac{dz}{R^{1+\frac{3}{\alpha}}}.$

Thus, the resistance to blood flow for Ellis fluid in a stenosed artery can be given as

$$\lambda = \frac{2L}{Q R_0^{1+\frac{1}{\alpha}}} \left(\frac{(\alpha+3)\mu_0 Q}{\rho u_0} \tau_{1/2}^{\alpha-1} \right)^{1/\alpha} [(2 - 2L_0) + I] \quad (7.13)$$

Using Gauss Quadrature two point integral formula, we compute the integral I as

$$I = \frac{2L_0}{\left(1 - ae^{-\frac{b}{3}L^2L_0^2} \right)^{1+\frac{3}{\alpha}}} \quad (7.14)$$

7.4 NUMERICAL RESULTS AND DISCUSSIONS

In this part of the paper, we have discussed the graphical features of pertinent parameters on flow characteristics such as blood flow rate, skin friction and resistance to blood flow. The effect of parameters α , a , $\tau_{1/2}$ and μ_0 on the flow characteristics are shown in figures 7.2-7.12. Flow rate of blood and skin friction are affected only in the stenotic region of an artery, that causes the graph have been drawn only in the stenotic region of an artery. The variations on blood flow rate for different values of parameters α , a , $\tau_{1/2}$ and μ_0 have been shown in figure 7.2-7.5. From figure 7.2, it is observed that the flow rate decreases vaguely with increase of α and attains its minimum at the central line of artery. Figure 7.3 depicts that the variation of flow rate with axial distance for different values of a . It is noticed that the flow rate decreases significantly with increase of a . Therefore it can be said that blood flow rate decreases with increase of stenosis height and attains its minimum at the stenosis throat. The variation of blood flow rate with axial distance for different values of $\tau_{1/2}$ is shown in figure 7.4. From here, it is found that the blood flow rate decreases with an increase of $\tau_{1/2}$ i.e. flow rate is maximum at lower value of shear stress at which $\mu = \mu_0/2$. The variations of flow rate along the axial distance for different values of μ_0 are shown in figure 7.5. It reveals that with μ_0 increasing, the blood flow rate diminishes. Therefore it is concluded that the blood flow rate decreases with increase of parameters α , a , $\tau_{1/2}$ and μ_0 .

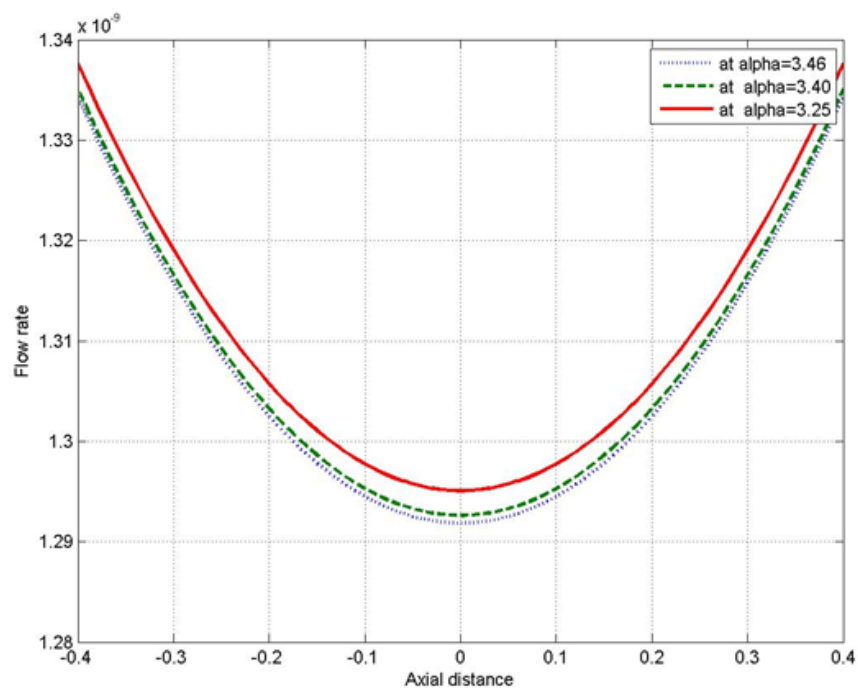


Fig. 7.2: Variation of flow rate with axial distance for different α .

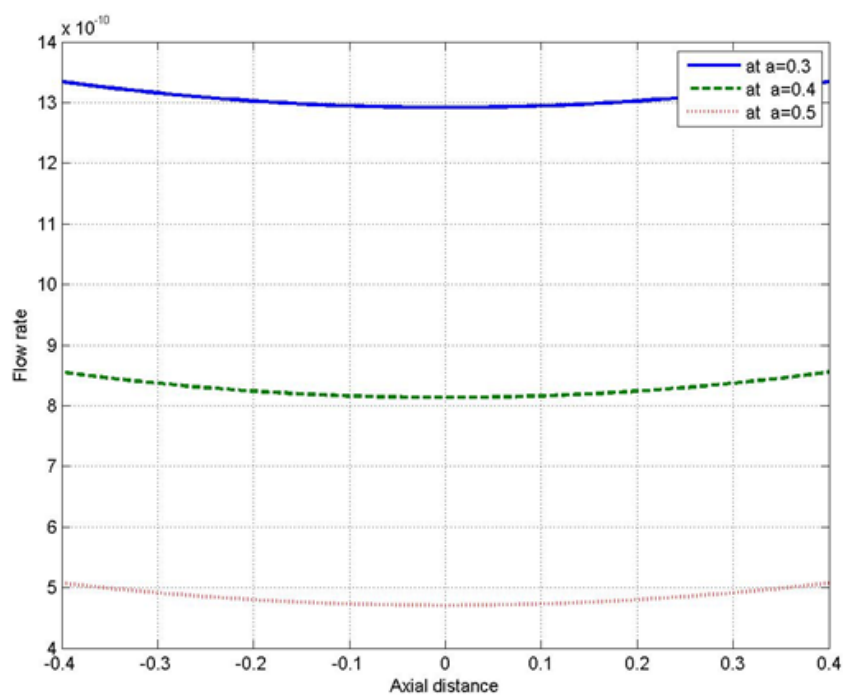


Fig. 7.3: Variation of flow rate with axial distance for different a .

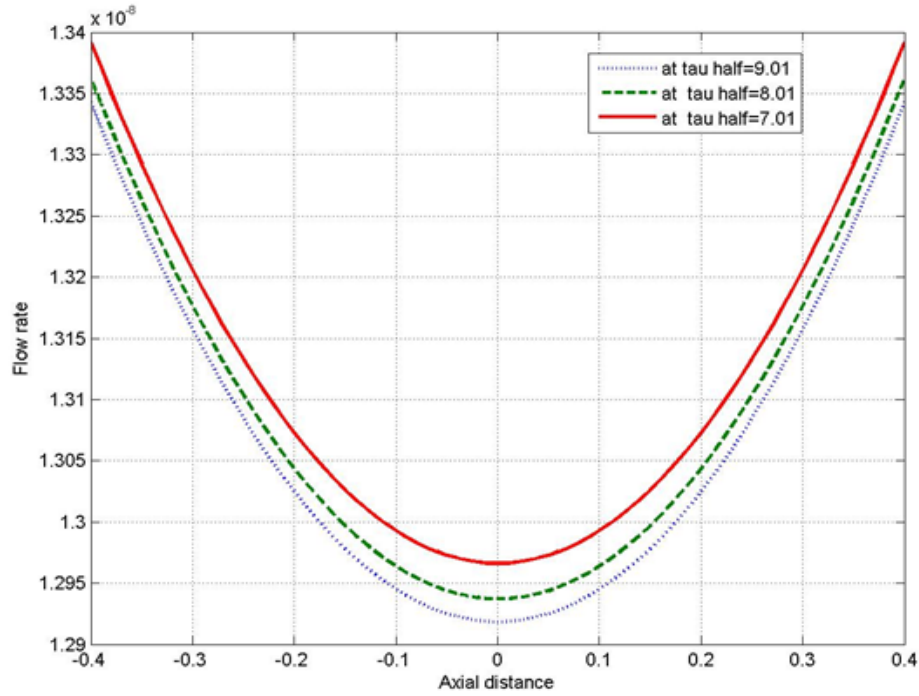


Fig. 7.4: Variation of flow rate with axial distance for different $\tau_{1/2}$.

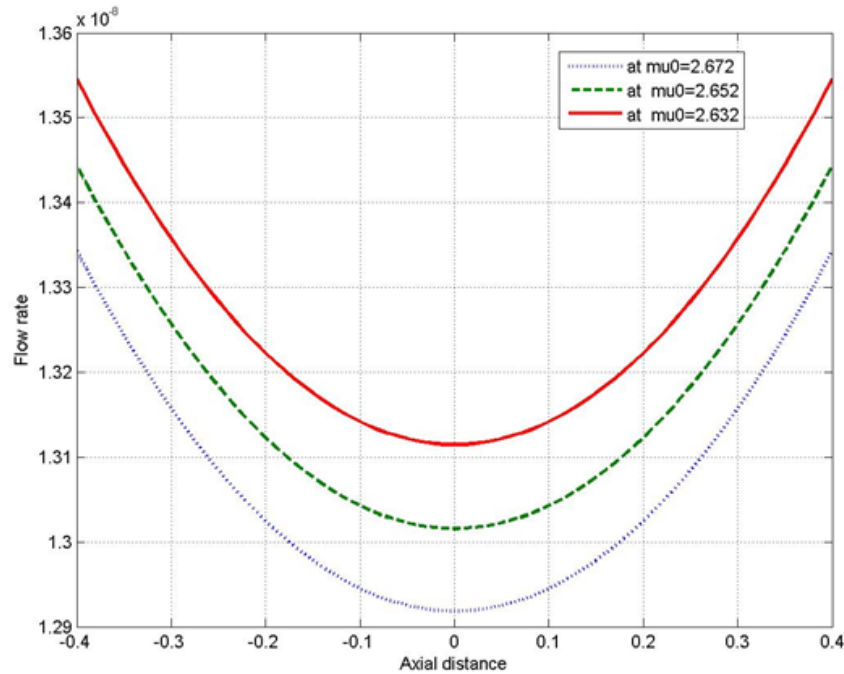


Fig. 7.5: Variation of flow rate with axial distance for different μ_0 .

The effects of stenosis on skin friction are discussed through figures 7.6-7.9. The variations of skin friction along the axial distance for different values of α are shown in figure 7.6. The graphs in figure 7.6 have been drawn for fix values of parameters ($\tau_{1/2} = 9.01$, $\mu_0 = 2.672$) of Ellis fluid. It ensures that the skin friction τ_R decreases as α decreases. Also it is noticed that the skin friction is maximum at the throat of stenosis and minimum at the onset of arterial stenosis. The variation of skin friction with axial distance for different values of a is plotted in figure 7.7. It is observed that the skin friction increases with the increase of values of a i.e. the skin friction is higher at the higher value of stenosis depth. In figure 7.8, the graphs have been drawn between the skin friction and axial distance of an artery for different values of $\tau_{1/2}$. It is noticed that the skin friction decreases as decrease the value of $\tau_{1/2}$ i.e. the skin friction attains its maximum at the large value of $\tau_{1/2}$. The variations of skin friction with the axial distance for different values of μ_0 are shown in figure 7.9. It shows that the skin friction τ_R increases as

increase of values of μ_0 . Therefore it is concluded that the skin friction decreases with decrease of parameters α , a , $\tau_{1/2}$ and μ_0 . Also it is observed that the skin friction attains its maximum at stenosis throat and minimum at the onset of the arterial stenosis. The same results are obtained by Venkatesan et al. [2013] with Casson fluid model, Misra et al. [2006] for Herschel-Bulkey fluid; and Sriyab [2014] for K-L fluid with bell-shaped mild arterial stenosis.

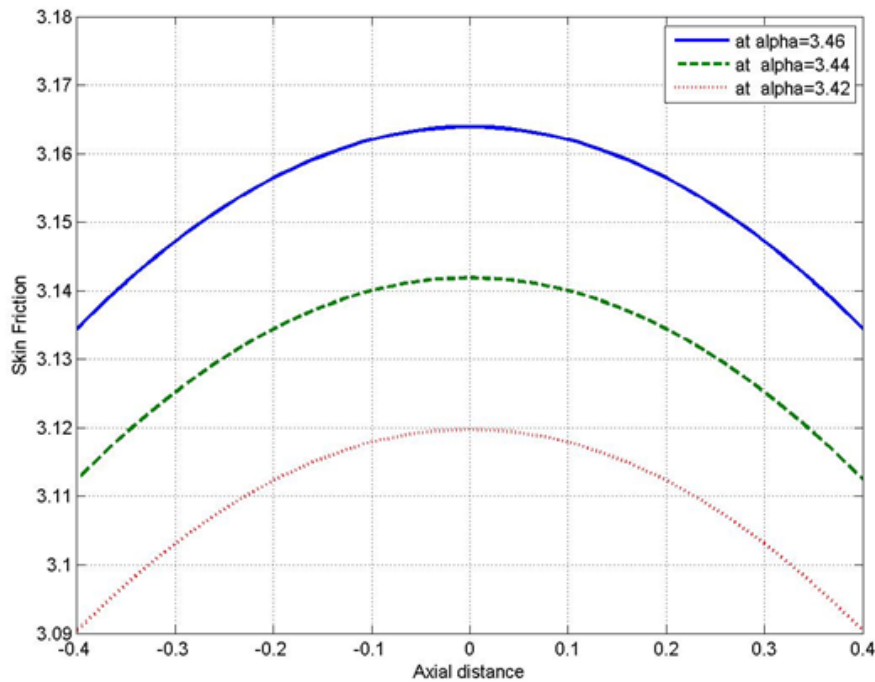


Fig. 7.6: Variation of skin friction with axial distance for different α .

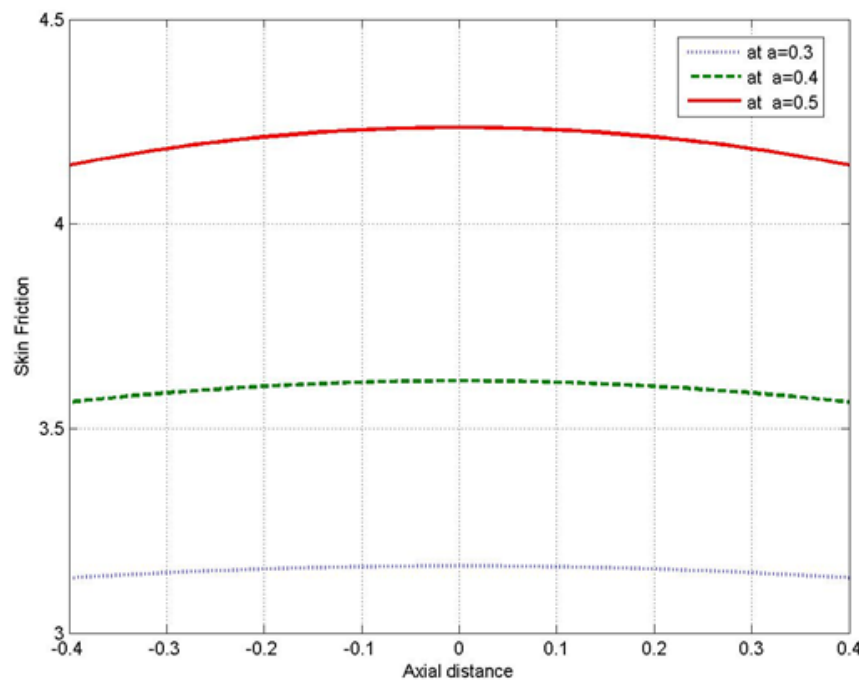


Fig. 7.7: Variation of skin friction with axial distance for different a .

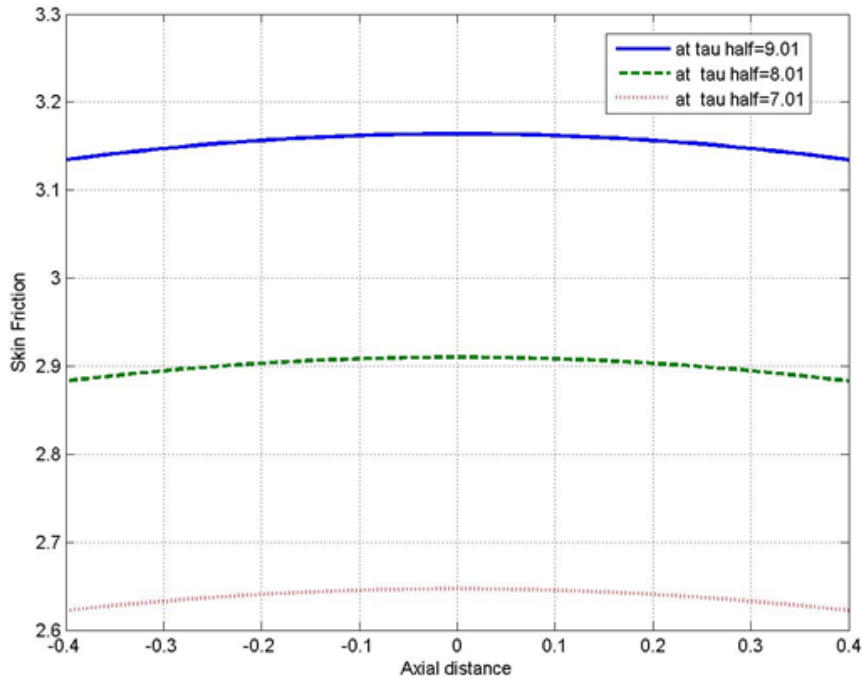


Fig. 7.8: Variation of skin friction with axial distance for different $\tau_{1/2}$.

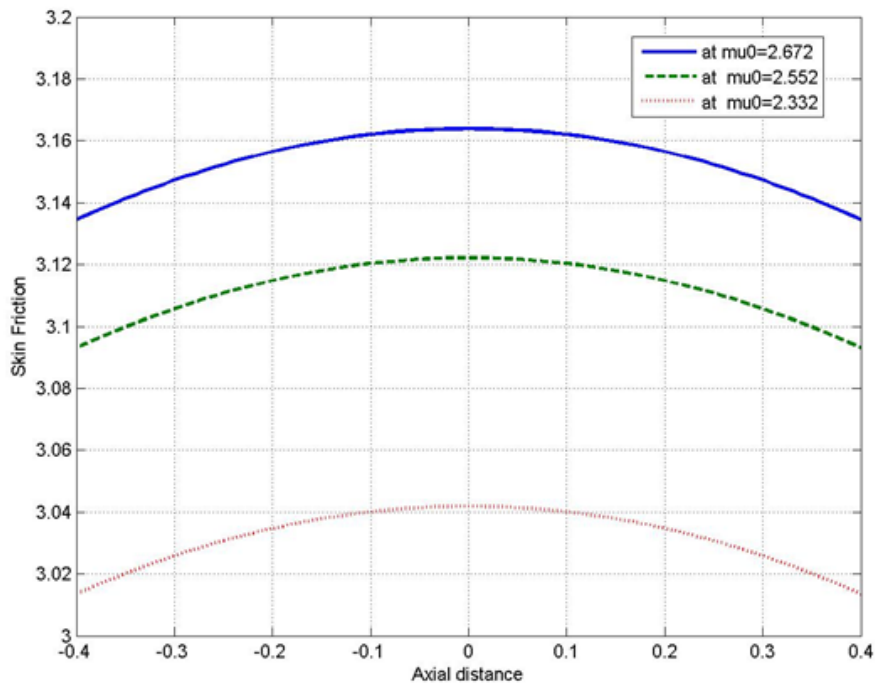


Fig. 7.9: Variation of skin friction with axial distance for different μ_0 .

The effects of stenosis on resistance to blood flow are discussed through figures 7.10-7.12. The variations of flow resistance with the stenosis depth for different values of L_0 are shown in figure 7.10. It is found that the resistance to blood flow increases non-linearly with the increase of stenosis height and stenosis length. In figure 7.11 the graphs have been drawn between the resistance to blood flow and stenosis depth for different values of α . It is observed that with the increase of α , resistance to blood flow decreases. The variations of flow resistance with the stenosis height for different values of $\tau_{1/2}$ are shown in figure 7.12. From here it is noticed that the resistance to blood flow decreases with decrease of $\tau_{1/2}$. Thus, it is concluded that the flow resistance of blood decreases with decrease of stenosis length L_0 and $\tau_{1/2}$. And it is noticed that flow resistance decreases with increase of indicial parameter α of Ellis fluid and increases with increase of arterial stenosis depth.

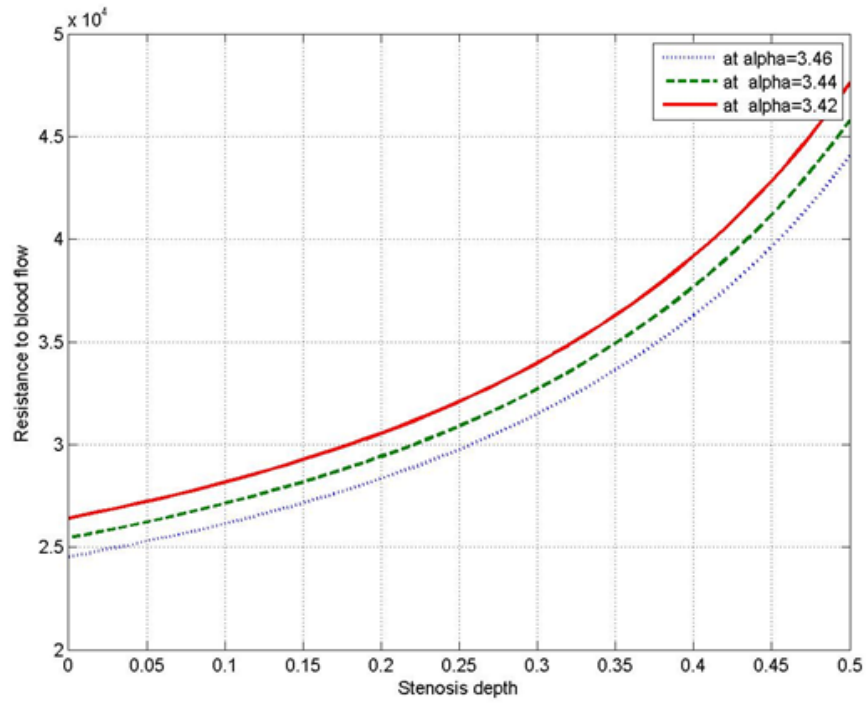


Fig. 7.10: Variation of resistance to blood flow for different α .

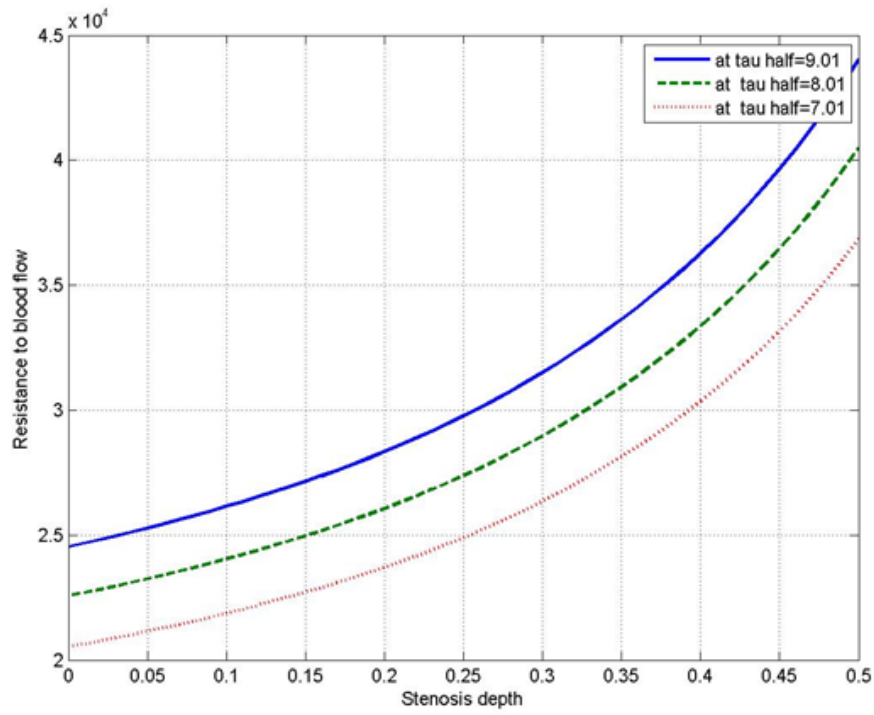


Fig. 7.11: Variation of resistance to blood flow for different $\tau_{1/2}$.

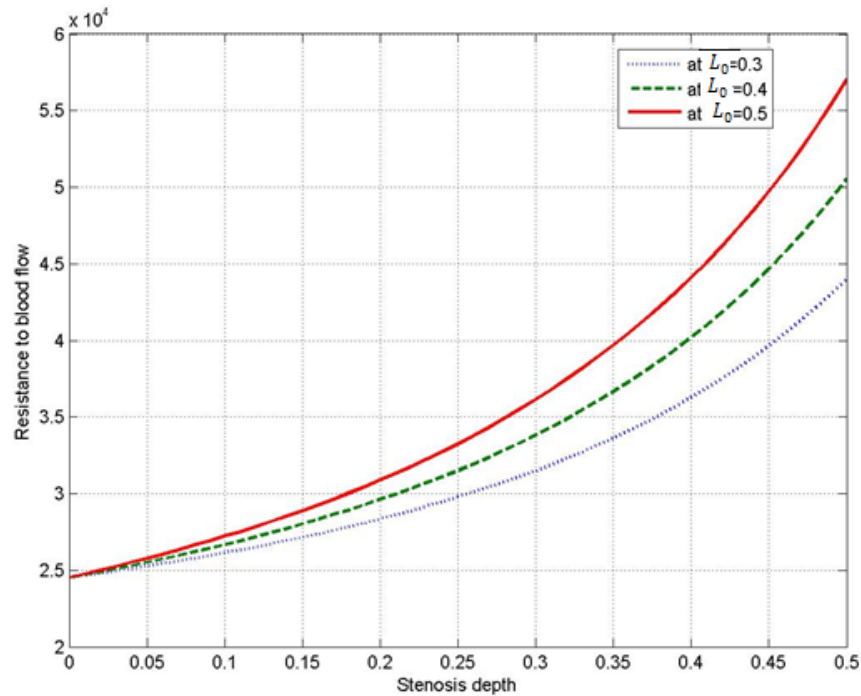


Fig. 7.12: Variation of resistance to blood flow for different L_0 .

7.5 CONCLUSIONS

The present study analyzed the steady flow of blood in a narrow artery with bell-shaped mild stenosis, treating blood as Ellis fluid and results are compared with the results of Venkatesan [2013], Misra *et al.* [2006] and Sriyab [2014]. The solution of the governing equations is solved analytically and numerically. The results for the resistance to blood flow, skin friction and blood flow rate are discussed through graphs for various physical parameters of the Ellis fluid model. To the best of our knowledge, no such analysis is available in the literature which can describe the effects of non-Newtonian Ellis fluid in arterial blood flow through bell-shaped mild stenosis. The present study shows that the skin friction and resistance to blood flow are maximum at the throat of the stenosis and minimum at the onset of the normal portion of the artery. Also it is concluded that the blood flow rate is maximum at the onset of stenosis and minimum at the throat of the stenosis. An increase in the size of stenosis cause to the resistance to blood flow through arteries in the brains, heart and other organs of the body.

Source of support: Nil, Conflict of interest: None Declared.

[Copy right © 2017. This is an Open Access article distributed under the terms of the International Journal of Mathematical Archive (IJMA), which permits unrestricted use, distribution, and reproduction in any medium, provided the original work is properly cited.]